IEEE Access
Multidisciplinary ⋮ Rapid Review ⋮ Open Access Journal

Received December 13, 2019, accepted December 20, 2019, date of publication December 25, 2019, date of current version January 10, 2020.

Digital Object Identifier 10.1109/ACCESS.2019.2962160

Frequency Agile Microstrip Patch Antenna Using an Anisotropic Artificial Dielectric Layer (AADL): Modeling and Design

JORGE L. SALAZAR-CERRENO[1,2], (Senior Member, IEEE), ZEESHAN QAMAR[2], (Member, IEEE), SHAHROKH SAEEDI[1,2], (Senior Member, IEEE), BINBIN WENG[1], (Member, IEEE), AND HJALTI S. SIGMARSSON[1,2], (Senior Member, IEEE)

[1]School of Electrical and Computer Engineering, The University of Oklahoma, Norman, OK 73072, USA
[2]Advanced Radar Research Center (ARRC), The University of Oklahoma, Norman, OK 73072, USA

Corresponding author: Jorge L. Salazar-Cerreno (salazar@ou.edu)

This work was supported by the U.S. Department of Defense, Office of Naval Research (DOD-ONR) under Grant N00014-18-1-2035, and in part by the Office of Navy Research (ONR) under Grant 1532140.

ABSTRACT This paper presents the modeling and design of a frequency agile antenna using an anistropic artificial dielectric layer (AADL) for multi-band phased array radar applications. The proposed AADL material is placed underneath the patch radiator and is designed using periodically arranged metallic cylinders in which varying height, diameter, and the distance used between them allows the control of the effective permittivity of the patch antenna. Closed form design expressions are formulated to synthesize the dielectric properties of the AADL as a function of the cylindrical unit cell dimensions. Design trade-offs based on the proposed formulation and numerical simulations show the overall performance of the AADL on microstrip patch (MS) antennas. To validate the proposed concept, five individual AADL MS patch antennas in C-band were designed, fabricated, and tested. Simulated and measured results (*s*-parameters and radiation patterns) are in good agreement with the results obtained from the theoretical model. The proposed AADL concept has the potential to be used in the development of future reconfigurable tunable multiband antennas that use liquid metal to dynamically change the heights of the cylinders.

INDEX TERMS Anisotropic, artificial dielectric layer, low-profile antenna, microstrip patch antenna, multi-band antenna, reconfigurable, shared aperture array, tunable.

I. INTRODUCTION

Currently, multiple applications, including communications, electronic warfare, weather radar, aircraft surveillance, security, and defense, require diverse type of antennas to cover from low frequencies to millimeter waves [1]. As the incorporation of new advanced sensors for these applications increases, platforms get crowded and limited in space and prime power. Moreover, adding more antenna apertures introduces new challenges such as increased radar cross-section (RCS), radio frequency (RF) blockage, and electromagnetic interference in communication and radar systems [1]. This enforces stringent requirements on system design specially for military applications. Multi-function, shared aperture, and reconfigurable capabilities reduce the number of RF systems needed during deployment and allow improved mobility and operational agility, while maintaining high spectral efficiency. Compact shared aperture array designs are required to enable efficient integration of shipboard RF functions including radar, communications, and electronic warfare (EW) [1]–[6].

Recently, new antenna designs that offer features to achieve reconfigurable radiation patterns, polarization, and frequency diversity [7]–[15], and/or their combinations [16]–[19], have been demonstrated. These antennas can be used to satisfy current and future commercial and military requirements. However, such antennas have multiple constraints that increase size, cost, and complexity. Additionally, array antennas for multiband applications must achieve good impedance match and high efficiency throughout all operation bands. In the

The associate editor coordinating the review of this manuscript and approving it for publication was Chan Hwang See.

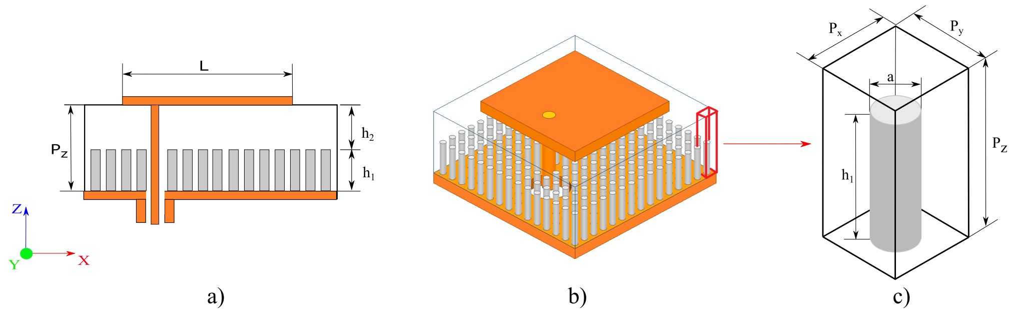

FIGURE 1. **Proposed AADL based antenna: a) Side view. b) 3D View. c) AADL unit cell.**

case of frequency reconfigurability, antennas should also exhibit a constant radiation pattern and consistent polarization performance across the entire frequency tuning range. For reconfigurable and multiband arrays, this requirement is difficult to achieve, since the element spacing is frequency dependent. Research articles that discuss reconfigurable and agile beam patterns for multiband applications can be found in [20]–[25]. The proposed architectures use MEMS switches and PIN diodes to achieve shared and reconfigurable features on an array. However, these antennas produce different radiation patterns at different frequencies. Arrays for large conical scanned angles ($\pm 60^o$) require an element spacing not larger than $0.5\lambda_o$ to avoid grating lobes. Grating lobes deteriorate the performance of a multi-band array, especially for the low portion of the frequency range. This problem is discussed in [26], where a switch based L/S frequency band adaptive antenna aperture is replaced with non-adaptive elements (works at S-band) in the antenna array.

Theoretical and numerical analysis of artificial dielectric layers (ADLs) for microwave substrates and multiple experiments using anisotropic materials for antenna applications are presented in [27]–[31]. It is important to mention that previous research on AADL's structures has not been done or applied for multiband antenna array application. To achieve frequency reconfigurable antennas, ferrite material was used as a substrate to tune a desired frequency by changing magnetic fields [32], [33]. However, these antennas had low efficiency and distorted radiation patterns. Liquid crystal material was also used for the same purpose [34], [35], but produced a very narrow frequency tuning range.

In this paper, an alternative approach to obtaining a reconfigurable and shared aperture array antenna is discussed. Instead of using an adaptive aperture element, an anisotropic artificial dielectric layer (AADL) on a radiating antenna is used. This AADL enables adaptive permittivity that allows changing the resonant frequencies, while the element dimensions and spacing remain unchanged. This concept provides invariant radiation characteristics of the array at different frequencies while maintaining the same aperture size and element spacing. Closed-form design equations to synthesize the AADL unit cell are presented. The proposed AADL is based on a metal-loaded dielectric that effectively changes the dielectric constant of the antenna substrate, allowing the use of same antenna for different frequency operations. To validate the proposed formulation, five antenna prototypes are designed, fabricated, and tested. This formulation enables efficient design methodology for reconfigurable array antennas that will facilitate the implementation of multiband and multifunction phased array systems that reduce the overall number of sensors in crowded platforms.

II. PROPOSED AADL ANTENNA AND FORMULATION

The geometry of the AADL unit cell proposed is composed by a host substrate with loaded metallic cylinders and its use to design a microstrip patch antenna is discussed in this section. Closed form design expressions are derived to synthesize the dielectric properties of the AADL as a function of the cylindrical unit cell dimensions.

A. AADL SUBSTRATE UNIT CELL

As illustrated in Figure 1c, the dimensions of the cylinder can be altered to change the host substrate in order to achieve different permittivities. The effective permittivity (ϵ_z) can be calculated by using the proposed piece-wise analytical expression in (1) and (2). These equations are obtained by using the curve fitting technique based on a parametric analysis.

$$\epsilon_z = (\epsilon_r - 0.04)e^{f_v} + 0.04e^{(\epsilon_r + F)f_v} \tag{1}$$

where

$$F = 371.55\left(\frac{a}{P_{x,y}}\right)^2 - 503\left(\frac{a}{P_{x,y}}\right) + 0.0821\left(\frac{a}{P_{x,y}}\right)^{-3.594} + 185 \tag{2}$$

$P_{x,y}$ (P_x or P_y) are the dimensions of the unit cells that represent the spacing between cylinders, and P_z is the overall dielectric thickness of the AADL. The proposed formulation works for symmetric AADL unit cell, i.e $P_x = P_y$. The volume of the cylinder is $f_v = \pi(a/P_{x,y})^2 h_1/(4\ P_z)$, where a and h_1 are the diameter and height. This formulation was used to design two AADL structures in which metallic vias were placed into two different host materials with relative permittivities of $\epsilon_r = 2.2$ and 3.48 respectively. A cylinder

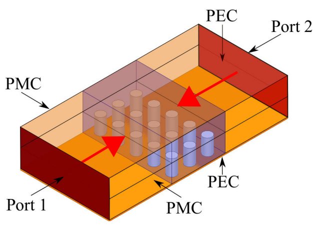

FIGURE 2. AADL geometry with PEC/PMC boundary conditions to extract ϵ_z. *s*-parameters are obtained using de-embedding ports, indicated by arrows in red.

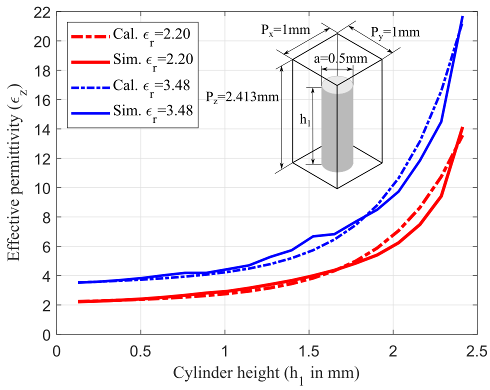

FIGURE 3. Calculated and simulated effective permittivity (ϵ_z) vs. the cylinder's height using different dielectric hosts ($\epsilon_r = 2.2$ and $\epsilon_r = 3.48$).

with a $a = 0.5$ mm diameter and a material thickness of $P_z = 2.413$ mm is used. To validate the proposed equations, AADL unit cells with different dielectric hosts were simulated in Ansys HFSS. Figure 2 illustrates the proposed unit cell with the required perfect electric (PEC) and perfect magnetic (PMC) boundary conditions for a HFSS simulation setup. Length of red-arrow is representing the distance of de-embed port into the proposed model. The constitutive parameters of the AADL structure (ϵ_z) are extracted using the Smith algorithm proposed in [36]. The comparative results of the effective permittivity as a function of the cylinder height using the proposed formulations (1)-(2), and simulated results in HFSS are shown in Figure 3. This figure shows good agreement between calculated and simulated results.

B. AADL ANTENNA

The proposed antenna geometry with the anisotropic AADL structure is illustrated in Fig.1. Periodic metallic cylinders are inserted in the antenna dielectric layer to convert an isotropic substrate to an anisotropic substrate with a dielectric property is frequency dependent. The height, diameter, and separations between cylinders are used to synthesize the permittivity as a function of the frequency of the AADL. To model the microstrip patch antenna with an AADL substrate, a conventional cavity model is used [37], [38]. This model is composed of top and bottom perfect electrical conductor (PEC) walls and side perfect magnetic conductor (PMC) walls in order to generate the dominant TM-mode where ϵ_z is sensitive to the AADL structure proposed.

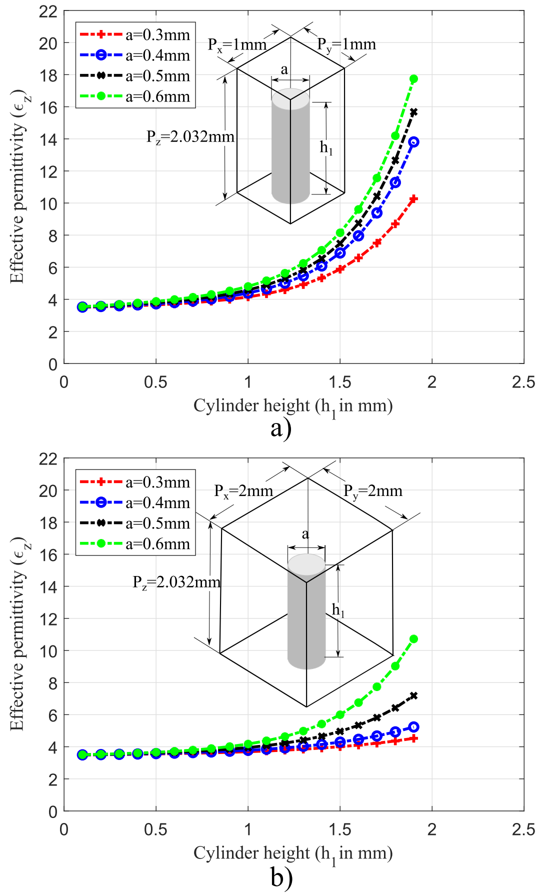

FIGURE 4. Calculated effective permittivity (ϵ_z) vs. cylinder's height using a dielectric host of $\epsilon_r = 3.48$ for different diameters ($a = 0.3$ mm to 0.6 mm). a) $P_{x,y} = 1$ mm. b) $P_{x,y} = 2$ mm.

The resonant frequency of the dominant TM-mode for the proposed AADL based antenna can be calculated using (3) to (6) [38].

$$f_{mnl} = \frac{c}{2\pi\sqrt{\epsilon_z}}\sqrt{\left(\frac{m\pi}{W_e}\right)^2 + \left(\frac{n\pi}{L_e}\right)^2 + \left(\frac{l\pi}{h}\right)^2} \quad (3)$$

where

$$\begin{cases} W_e = W \\ L_e = L + 2\Delta L = L[1+\delta(L)]\dfrac{\sqrt{\epsilon_{eL}\epsilon_{eW}}}{\epsilon_z} \end{cases} \quad (4)$$

$$\delta L = \frac{h}{L}\left(0.882 + 0.162\frac{(\epsilon_z - 1)}{\epsilon_z^2} + \frac{\epsilon_z + 1}{\pi\epsilon_z}\left[0.758 + \ln\left(\frac{L}{h} + 1.88\right)\right]\right) \quad (5)$$

$$\epsilon_{eL,eW} = \frac{1}{2}\left[(\epsilon_z + 1) + (\epsilon_z - 1)\left(1 + \frac{10h}{L, W}\right)^{-0.5}\right] \quad (6)$$

W and L are the physical dimensions of a patch antenna, and W_e and L_e are the electrical dimensions of the patch antenna. $\epsilon_{eL,eW}$ represents the effective dielectric constant in the z-axis that is dependent on ϵ_z, L, W and h.

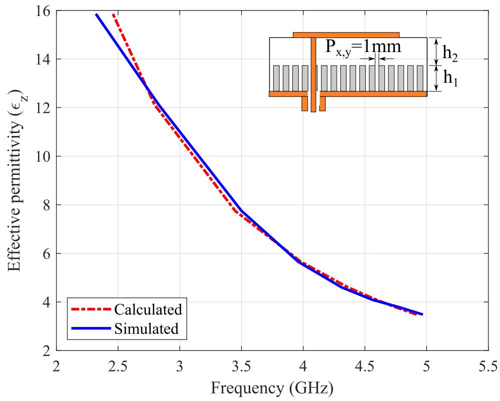

FIGURE 5. Effective permittivity (ϵ_z) vs. resonant frequency of AADL MS patch antenna ($L = W = 14.7$ mm) with different cylinder's height, diameter $a = 0.5$ mm and distance ($P_{x,y}$) of 1 mm between them in a dielectric host $\epsilon_r = 3.48$.

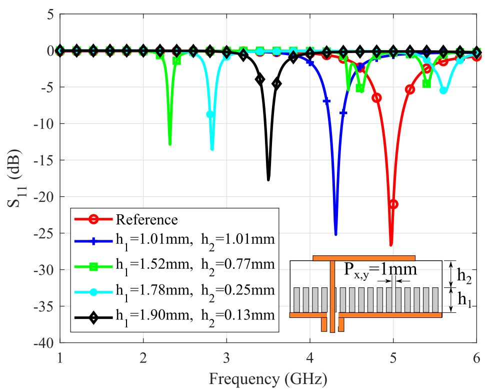

FIGURE 6. Simulated *s*-parameters vs. resonant frequency of AADL MS patch antenna ($L = W = 14.7$ mm) with different cylinder's height, diameter $a = 0.5$ mm and distance ($P_{x,y}$) of 1 mm between them in a dielectric host $\epsilon_r = 3.48$.

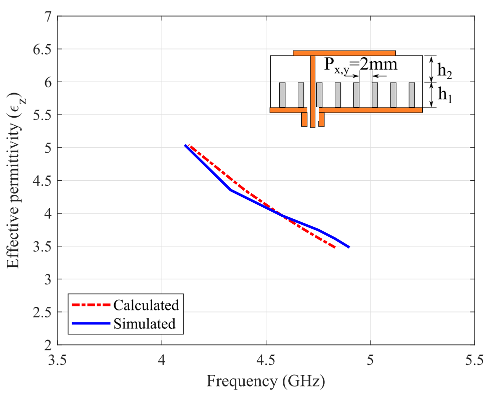

FIGURE 7. Effective permittivity (ϵ_z) vs. resonant frequency of AADL MS patch antenna ($L = W = 14.7$ mm) with different cylinder's height, diameter $a = 0.5$ mm and distance ($P_{x,y}$) of 2 mm between them in a dielectric host $\epsilon_r = 3.48$.

III. DESIGN TRADE-OFFS

Using (1)-(2), the effective permittivity of the MS patch antenna (ϵ_z) is calculated for different cylinder dimensions (radius, height, and spacing). Roger Duroid 4350B with a

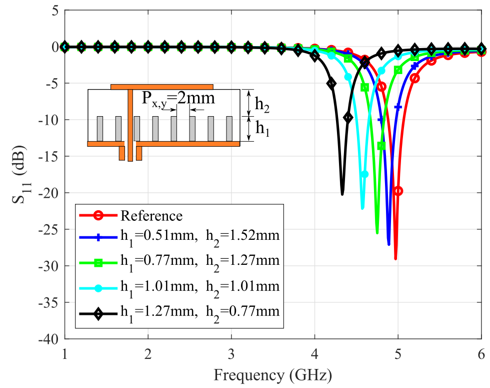

FIGURE 8. Simulated *s*-parameters vs. resonant frequency of AADL MS patch antenna ($L = W = 14.7$ mm) with different cylinder's height, diameter $a = 0.5$ mm and distance ($P_{x,y}$) of 2 mm between them in a dielectric host $\epsilon_r = 3.48$.

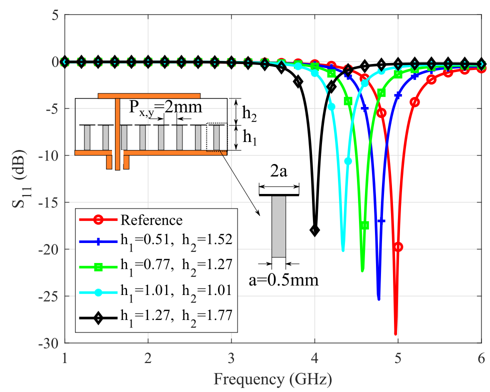

FIGURE 9. Simulated *s*-parameters of the AADL based MS square patch antenna ($L = W = 14.7$ mm) after the inclusion of conducting rings onto the cylinders.

relative permittivity of $\epsilon_r = 3.48$ was used at different thicknesses (P_z) to demonstrate this formulation and highlight the benefits of the proposed AADL structure in a multiband antenna. The lower effective permittivity value of the AADL is 3.48 and increases as the height of the metallic cylinder increases. This is due to the high density of metallic cylinder in a 2D lattice metallic array that increase the capacitive storage energy. As illustrated in Figure 3, a unit cell with $P_{x,y} = 1$ mm and cylinder diameter of 0.5 mm produces an effective permittivity that varies from 2.2 to 14 for a host material with $\epsilon_r = 2.2$, and an effective permittivity that varies from 3.48 to 21.6 for a host material with $\epsilon_r = 3.48$ and overall height of 2.032 mm. Increasing the unit cell size to $P_{x,y} = 2$ mm (see Figure 4) reduces the permittivity range from 3.48 to 5.12. This is due to the low density of metallic structure in a 2D lattice metallic array that reduce the capacitive storage energy of the proposed AADL strcuture. Another variable that can be used to change the effective permittivity is the diameter of the cylinder. Figure 4 shows the cases of using unit cells of 1 mm and 2 mm that have different cylinder diameters ranging from 0.3 mm to 0.6 mm. The larger the cylinder diameter, the greater the effective

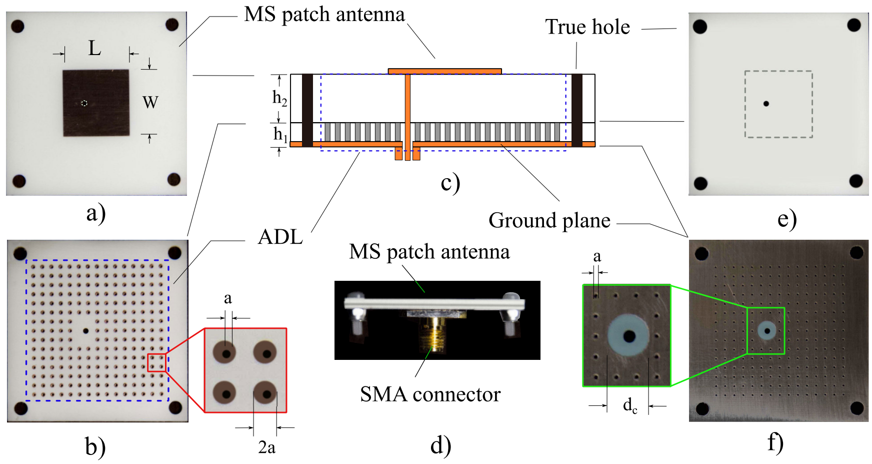

FIGURE 10. Prototype of the proposed AADL based frequency agile MS square patch antenna a) Top layer b) Bottom layer with AADL geometry. c) Side view of the proposed AADL based patch model. d) Side view of the AADL with an SMA connector. e) Bottom layer of top sub-dielectric. f) Bottom layer of bottom sub-dielectric. (Dimensions: $L = W =$ 14.7 mm, $a = 0.5$ mm and $dc = 4.25$ mm.

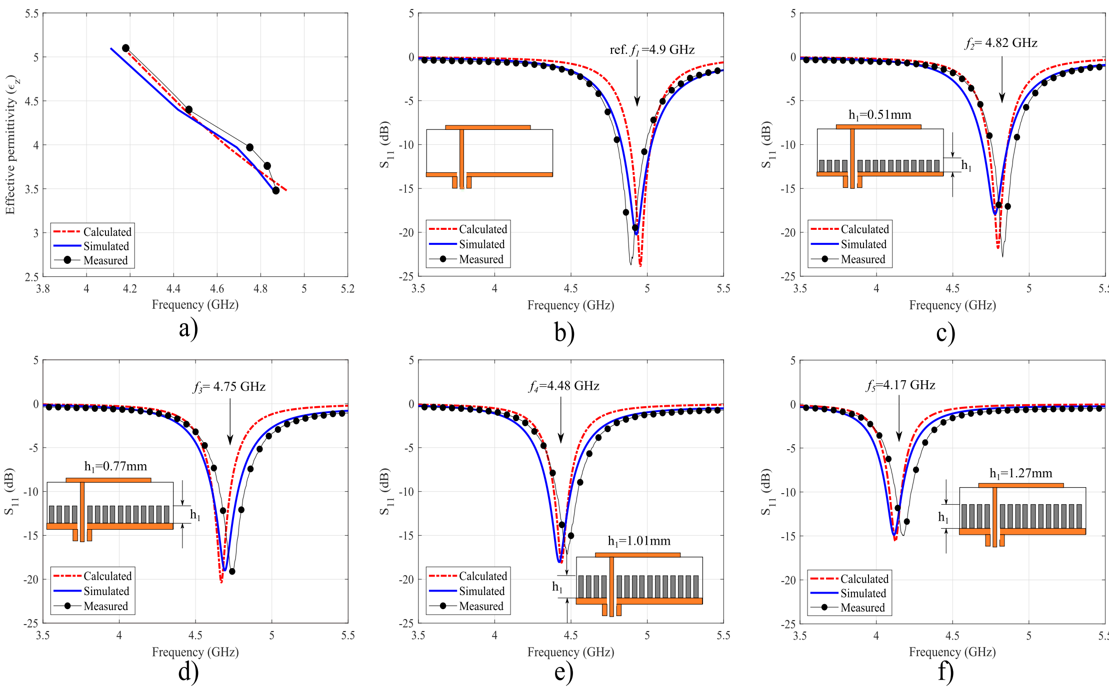

FIGURE 11. Calculated, simulated, and measured results of the proposed AADL MS square patch antenna a) Frequency vs. effective permittivity (ϵ_z) b) Reference c) $h_1 = 0.51$ mm, $h_2 = 1.52$ mm d) $h_1 = 0.77$ mm, $h_2 = 1.27$ mm e) $h_1 = 1.01$ mm, $h_2 = 1.01$ mm f) $h_1 = 1.27$ mm, $h_2 = 0.77$ mm.

permittivity that can be obtained. Figure 4 also shows the tunable capability of the AADL proposed as a function of the metallic cylinder height. Liquid metal can be used to dynamically reconfigure cylinder height in order to have a tunable AADL in the proposed antenna.

Figure 5 illustrates the calculated and simulated results of the effective permittivity (ϵ_z) underneath of a MS patch antenna as a function of frequency. Cylinders heights (h_1) from 0.51 mm to 1.27 mm are changed to obtain an effective permittivity from 3.48 to 15.8 when the frequency of the source are changed from 2.3 GHz to 4.9 GHz. In this particular case, the design includes a cylinder radius of 0.5 mm, AADL unit cell size ($P_{x,y}$) are 1 mm. Numerical simulation in HFSS is performed to evaluate the impedance frequency response of the AADL antenna. Figure 6 illustrates the simulated results of the reflection coefficient (S11 in dB) versus frequency for the AADL antenna for different cylinders heights (h_1). changing the high cylinders heights (h_1) from 0.51 mm to 1.27 mm, the resonance frequency the antenna change from 4.9 GHz to 4.34 GHz. Figure 6 also shows the

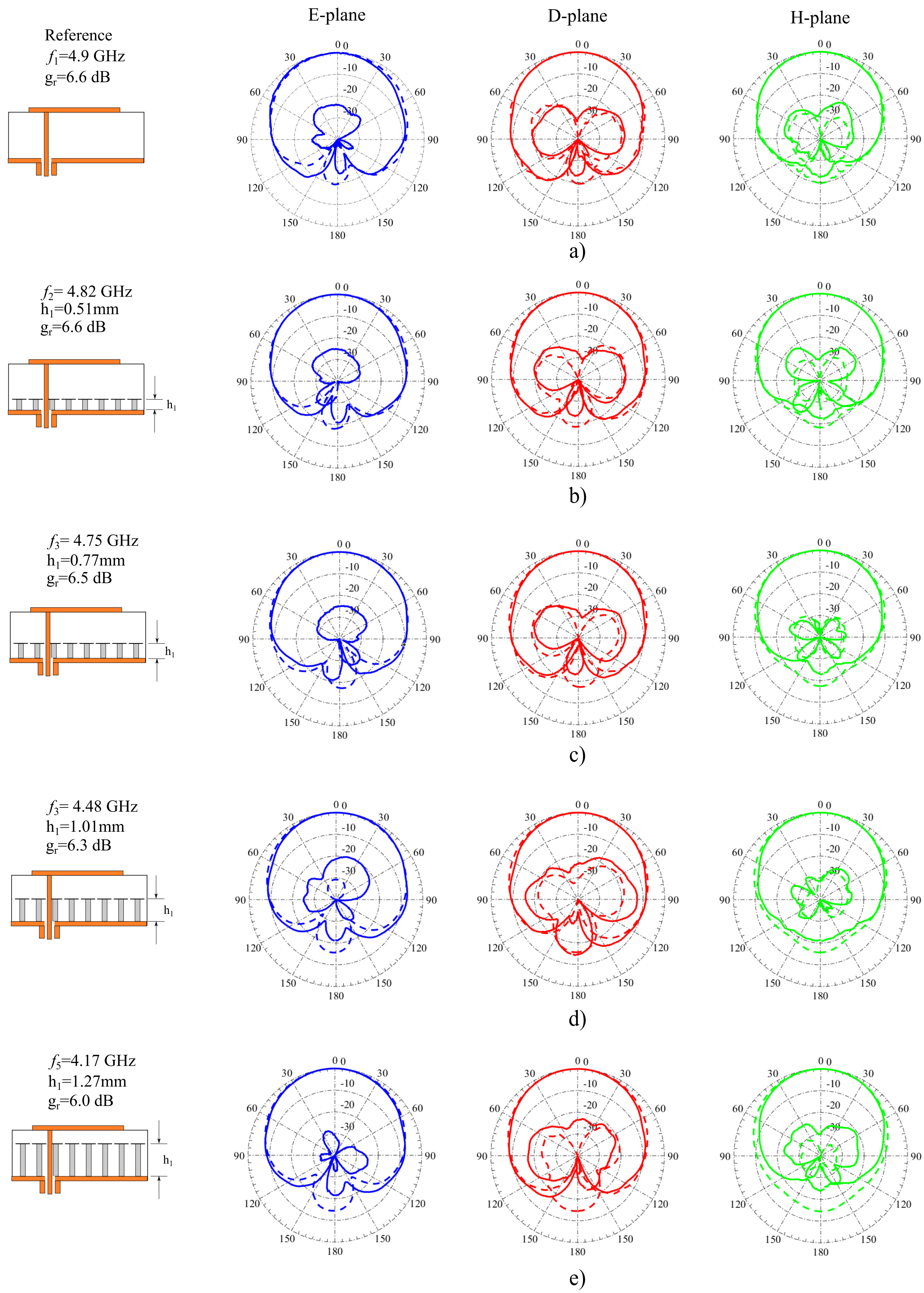

FIGURE 12. **Simulated (dashed) and measured (solid) radiation patterns of the proposed AADL MS square patch antennas. a) Reference, b) $h_1 = 0.51$ mm, $h_2 = 1.52$ mm c) $h_1 = 0.77$ mm, $h_2 = 1.27$ mm d) $h_1 = 1.01$ mm, $h_2 = 1.01$ mm e) $h_1 = 1.27$ mm, $h_2 = 0.77$ mm. Blue represents the E-plane, red represents the D-plane, and green represents the H-plane. Simulated realized gain from 6.0 dB to 6.6 dB was obtained for frequency range from 4.17 GHz to 4.0 GHz.**

S11 decreases as the frequency increases, this is attributed to the narrow-band characteristic of the MS patch antenna, where the probe feed position is sensitivity to the coupling factor between the feed and antenna. This situation can be improved using MS patch with a different feed mechanism, for example using the proximity coupling of aperture coupled patch antenna or increasing the antenna impedance bandwidth using a parasitic patch antenna.

Figure 7 shows simulated and calculated results of AADL substrate with a unit cell where $P_{x,y}$ is increased to 2 mm. As it was expected, the effective permittivity offers a small range of operation from 3.48 to 5.12. Using this AADL substrate, simulated results of the reflection coefficient (S11 in dB) versus frequency for AADL MS patch antenna are illustrated in Figure 8. An AADL MS patch antenna with narrow range frequency of operation was obtained. Conducting rings with a diameter of $2a$ were added in the top of each cylinder to facilitate the PCB fabrication process. Comparing the results between the AADL MS patch antennas with and without conducting rings (see Figure 8 and Figure 9), can be observed. The conducting rings added a capacitive effect that compensates the inductive loading of the cylinders that typically increases for the lower frequencies. Tunable frequency range increase from 4.34 GHz −4.9 GHz to 4.17 GHz to 4.9 GHz.

IV. MEASURED RESULTS AND VALIDATION

Five C-band antenna prototypes were designed, fabricated, and tested to validate the proposed method. Figure 10 shows pictures of different layers of the proposed AADL MS square patch antenna. Figure 11 and Figure 12 show the geometries of each antenna with comparative results between calculated, simulated, and measured s-parameters and radiation patterns. The cylinder diameter (a) of 0.5 mm and spacing ($P_{x,y}$) of 2 mm are kept fixed for all cases. Circular metal plates of 1 mm diameter were placed on each cylinder to insure a proper fabrication process. For all AADL antenna cases, Rogers 4350B is used as a host dielectric layer. The first dielectric core (see top and bottom in Figure 10a and e) contains the square MS patch antenna. The second one (Figure 10b and f) contains the periodic AADL metallic cylinders. In all cases, both substrates were put together using four nonmetallic screws. Different material heights of the bottom and top layers of each antenna were used while keeping the overall thicknesses of the antennas constant (i.e. 2.032 mm).

1) *s*-PARAMETERS

The calculated, simulated and measured results are shown in Figure 11. The frequency range of the proposed AADL is from 4.17 GHz to 4.9 GHz and results from changing the permittivity of the AADL from 3.48 to 5.12, as shown in Figure 11a. The measured results varied slightly compared to the numerical and simulated results. This is attributed to a very small air gap between the dielectric layers and the slight off-center placement of the metallic disks above the cylinders. The variations may also be attributed to the variability of the dielectric constant of the host material, in this case, 3.48 ± 0.05 for Rogers 4350B. An antenna without an AADL was also fabricated and used as a reference (See Figure 11b). In all cases, the frequency response for the S11 parameters over a frequency range from 4.17 GHz to 4.9 GHz match well with the simulated and calculated responses using the proposed analytical model.

2) ANTENNA PATTERNS

The radiation patterns of five prototypes were measured in the far-field chamber at the Radar Innovation Laboratory at The University of Oklahoma. Co-polar and cross-polarization patterns of the five H-polarized MS patch antenna prototypes for E-, D-, and H-planes are obtained and compared with simulated results in HFSS (see Figure 12). The Ludwig-3 polarization definition is used for this antenna [39]. The antennas present the same behavior in beam-width and backlobe radiation. Therefore, the proposed AADL based antenna can provide invariant radiation characteristics for the entire frequency tuning range. Co-polar pattern shapes match very well with simulated results in all frequencies and planes. However, a discrepancy in the cross-polar patterns in the E-planes is observed. This discrepancy is attributed to the misalignment between the AUT and probe antenna during the measurements and cross-polarization contamination of the probe, since it is not rated for measurements below −35 dB.

V. CONCLUSION

In this work, a AADL based frequency agile reconfigurable antenna is proposed. This antenna uses a metal-loaded artificial material that effectively changes the dielectric constant of the antenna substrate, thus allowing the use of the same antenna for different frequency operations. Closed-form design equations to synthesize the AADL unit cell are presented. The accuracy and ease of use of these equations allow expediting the design process of the proposed antenna using reconfigurable AADLs.The proposed AADL material enables the use of the same aperture to achieve a multiband antenna with invariant radiation patterns. Simulated realized gain from 6.02 dB to 6.61 dB was observed for a frequency range from 4.17 GHz to 4.9 GHz, respectively. For proof of concept, several antenna prototypes limited frequency range (4.17 GHz to 4.9 GHz) are used. The simulations and measurements are in good agreement and in line with the behavior of the proposed theoretical model. This technique can be extended for other frequency bands. The proposed low profile architecture provides a wide tuning range with better efficiency and high cross-polarization isolation. The proposed AADL antenna concept has the potential to be used in the development of reconfigurable tunable multiband antennas that use liquid metal to dynamically change the heights of the cylinders.

ACKNOWLEDGMENT

The authors would like to thank J. Diaz, A. Stringer, and N. Aboserwal. Any opinions, findings, and conclusions or recommendations expressed in this material are those of the author(s), and do not necessarily reflect the views of the ONR.

REFERENCES

[1] G. Tavik, C. Hilterbrick, J. Evins, J. Alter, J. Crnkovich, J. De Graaf, W. Habicht, G. Hrin, S. Lessin, D. Wu, and S. Hagewood, "The advanced multifunction RF concept," *IEEE Trans. Microw. Theory Techn.*, vol. 53, no. 3, pp. 1009–1020, Mar. 2005.

[2] R. Mital, B. L. Rao, D. P. Patel, and G. C. Tavik, "Wideband multifunction array architectures using wavelength-scaled radiating elements," in *Proc. IEEE Int. Symp. Phased Array Syst. Technol.*, Oct. 2013, pp. 588–592.

[3] R. Kindt, R. Mital, J. Logan, and M. Vouvakis, "Dual-polarized sliced notch array—Ultra-wideband flares with exceptional polarization control," in *Proc. IEEE Int. Symp. Phased Array Syst. Technol. (PAST)*, Oct. 2016, pp. 1–5.

[4] R. Kindt, R. Mital, J. Logan, M. Lee, and M. Vouvakis, "A 6:1 Bandwidth PUMA array at 7 mm scale," in *Proc. IEEE Int. Symp. Phased Array Syst. Technol. (PAST)*, Oct. 2016, pp. 1–4.

[5] J. T. Logan, R. W. Kindt, M. Y. Lee, and M. N. Vouvakis, "Opportunities and advances in ultra-wideband electronically scanned arrays," in *Proc. IEEE Int. Symp. Antennas Propag. (APSURSI)*, Jun. 2016, pp. 431–432.

[6] R. W. Kindt and M. N. Vouvakis, "Analysis of a wavelength–scaled array (WSA) architecture," *IEEE Trans. Antennas Propag.*, vol. 58, no. 9, pp. 2866–2874, Sep. 2010.

[7] W. Lin, H. Wong, and R. W. Ziolkowski, "Wideband pattern–reconfigurable antenna with switchable broadside and conical beams," *IEEE Antennas Wireless Propag. Lett.*, vol. 16, pp. 2638–2641, 2017.

[8] W.-Q. Deng, X.-S. Yang, C.-S. Shen, J. Zhao, and B.-Z. Wang, "A dual–polarized pattern reconfigurable Yagi patch antenna for microbase stations," *IEEE Trans. Antennas Propag.*, vol. 65, no. 10, pp. 5095–5102, Oct. 2017.

[9] Y.-F. Cheng, X. Ding, B.-Z. Wang, and W. Shao, "An azimuth-pattern-reconfigurable antenna with enhanced gain and front-to-back ratio," *IEEE Antennas Wireless Propag. Lett.*, vol. 16, pp. 2303–2306, 2017.

[10] H. Wong, W. Lin, L. Huitema, and E. Arnaud, "Multi–polarization reconfigurable antenna for wireless biomedical system," *IEEE Trans. Biomed. Circuits Syst.*, vol. 11, no. 3, pp. 652–660, Jun. 2017.

[11] S.-L. Chen, F. Wei, P.-Y. Qin, Y. J. Guo, and X. Chen, "A multi-linear polarization reconfigurable unidirectional patch antenna," *IEEE Trans. Antennas Propag.*, vol. 65, no. 8, pp. 4299–4304, Aug. 2017.

[12] P. Zhang, Y. Cui, and R. Li, "A novel polarization reconfigurable circularly polarized antenna," in *Proc. IEEE Int. Symp. Antennas Propag. USNC/URSI Nat. Radio Sci. Meeting*, Jul. 2017, pp. 2215–2216.

[13] Y. Song, Q. Xu, Y. Tian, J. Yang, Y. Wu, X. Tang, and K. Kang, "An on–chip frequency–reconfigurable antenna For Q–band broadband applications," *IEEE Antennas Wireless Propag. Lett.*, vol. 16, pp. 2232–2235, 2017.

[14] W. Su, S. A. Nauroze, B. Ryan, and M. M. Tentzeris, "Novel 3D printed liquid-metal-alloy microfluidics-based zigzag and helical antennas for origami reconfigurable antenna 'trees,'" in *IEEE MTT-S Int. Microw. Symp. Dig.*, Jun. 2017, pp. 1579–1582.

[15] Y. K. Choukiker and S. K. Behera, "Wideband frequency reconfigurable Koch snowflake fractal antenna," *IET Microw., Antennas Propag.*, vol. 11, no. 2, pp. 203–208, Jan. 2017.

[16] M. Allayioti and J. R. Kelly, "Multiple parameter reconfigurable microstrip patch antenna," in *Proc. IEEE Int. Symp. Antennas Propag. USNC/URSI Nat. Radio Sci. Meeting*, Jul. 2017, pp. 1141–1142.

[17] S.-L. Chen, P.-Y. Qin, C. Ding, and Y. J. Guo, "Cavity–backed proximity–coupled reconfigurable microstrip antenna with agile polarizations and steerable beams," *IEEE Trans. Antennas Propag.*, vol. 65, no. 10, pp. 5553–5558, Oct. 2017.

[18] C. Ni, M. S. Chen, Z. X. Zhang, and X. L. Wu, "Design of frequency- and polarization–reconfigurable antenna based on the polarization conversion metasurface," *IEEE Antennas Wireless Propag. Lett.*, vol. 17, no. 1, pp. 78–81, Jan. 2018.

[19] S. N. M. Zainarry, N. Nguyen-Trong, and C. Fumeaux, "A frequency- and pattern–reconfigurable two–element array antenna," *IEEE Antennas Wireless Propag. Lett.*, vol. 17, no. 4, pp. 617–620, Apr. 2018.

[20] M. Shirazi, T. Li, J. Huang, and X. Gong, "A reconfigurable dual–polarization slot–ring antenna element with wide bandwidth for array applications," *IEEE Trans. Antennas Propag.*, vol. 66, no. 11, pp. 5943–5954, Nov. 2018.

[21] Y.-M. Cai, K. Li, Y. Yin, S. Gao, W. Hu, and L. Zhao, "A low–profile frequency reconfigurable grid–slotted patch antenna," *IEEE Access*, vol. 6, pp. 36305–36312, 2018.

[22] N. Nguyen-Trong, A. Piotrowski, L. Hall, and C. Fumeaux, "A frequency- and polarization–reconfigurable circular cavity antenna," *IEEE Antennas Wireless Propag. Lett.*, vol. 16, pp. 999–1002, 2017.

[23] F. Zadehparizi and S. Jam, "Increasing reliability of frequency–reconfigurable antennas," *IEEE Antennas Wireless Propag. Lett.*, vol. 17, no. 5, pp. 920–923, May 2018.

[24] C. Gu, S. Gao, B. Sanz-Izquierdo, E. A. Parker, W. Li, X. Yang, and Z. Cheng, "Frequency–agile beam–switchable antenna," *IEEE Trans. Antennas Propag.*, vol. 65, no. 8, pp. 3819–3826, Aug. 2017.

[25] Y. P. Selvam, M. Kanagasabai, M. G. N. Alsath, S. Velan, S. Kingsly, S. Subbaraj, Y. V. R. Rao, R. Srinivasan, A. K. Varadhan, and M. Karuppiah, "A low-profile frequency- and pattern-reconfigurable antenna," *IEEE Antennas Wireless Propag. Lett.*, vol. 16, pp. 3047–3050, 2017.

[26] N. Haider, A. G. Yarovoy, and A. G. Roederer, "L/S-band frequency reconfigurable multiscale phased array antenna with wide angle scanning," *IEEE Trans. Antennas Propag.*, vol. 65, no. 9, pp. 4519–4528, Sep. 2017.

[27] A. T. Hassan, M. A. Moharram Hassan, and A. A. Kishk, "Modeling and design empirical formulas of microstrip ridge gap waveguide," *IEEE Access*, vol. 6, pp. 51002–51010, 2018.

[28] P. I. Dankov, "Uniaxial anisotropy estimation of the modem artificial dielectrics for antenna applications," in *IEEE MTT-S Int. Microw. Symp. Dig.*, Sep. 2017, pp. 1–3.

[29] D. Cavallo, W. H. Syed, and A. Neto, "Closed-form analysis of artificial dielectric layers part i: Properties of a single layer under plane-wave incidence," *IEEE Trans. Antennas Propag.*, vol. 62, no. 12, pp. 6256–6264, Dec. 2014.

[30] D. Cavallo, W. H. Syed, and A. Neto, "Closed-form analysis of artificial dielectric layers—Part II: Extension to multiple layers and arbitrary illumination," *IEEE Trans. Antennas Propag.*, vol. 62, no. 12, pp. 6265–6273, Dec. 2014.

[31] A. G. Hadiwijaya and A. Munir, "Artificial dielectric material for lowering resonant frequency of microstrip circular patch antenna," in *Proc. Int. Symp. Intell. Signal Process. Commun. Syst. (ISPACS)*, Nov. 2015, pp. 556–559.

[32] A. Shamim, J. R. Bray, N. Hojjat, and L. Roy, "Ferrite LTCC–based antennas for tunable SoP applications," *IEEE Trans. Compon., Packag., Manuf. Technol.*, vol. 1, no. 7, pp. 999–1006, Jul. 2011.

[33] L.-R. Tan, R.-X. Wu, C.-Y. Wang, and Y. Poo, "Magnetically Tunable Ferrite Loaded SIW Antenna," *IEEE Antennas Wireless Propag. Lett.*, vol. 12, pp. 273–275, 2013.

[34] M. A. Christou, N. C. Papanicolaou, and A. C. Polycarpou, "A nematic liquid crystal tunable patch antenna," in *Proc. 8th Eur. Conf. Antennas Propag. (EuCAP)*, Apr. 2014, pp. 1875–1878.

[35] L. Liu and R. Langley, "Liquid crystal tunable microstrip patch antenna," *Electron. Lett.*, vol. 44, no. 20, p. 1179, 2008.

[36] D. R. Smith, W. J. Padilla, D. C. Vier, S. C. Nemat-Nasser, and S. Schultz, "Composite medium with simultaneously negative permeability and permittivity," *Phys. Rev. Lett.*, vol. 84, no. 18, pp. 4184–4187, Jul. 2002.

[37] F. Bouttout, F. Benabdelaziz, A. Benghalia, D. Khedrouche, and T. Fortaki, "Uniaxially anisotropic substrate effects on resonance of rectangular microstrip patch antenna," *Electron. Lett.*, vol. 35, no. 4, pp. 255–256, 1999.

[38] T.-W. Kim, J.-S. Park, and S.-O. Park, "A theoretical model for resonant frequency and radiation pattern on rectangular microstrip patch antenna on liquid crystal substrate," *IEEE Trans. Antennas Propag.*, vol. 66, no. 9, pp. 4533–4540, Sep. 2018.

[39] N. A. Aboserwal, J. L. Salazar, J. A. Ortiz, J. D. Diaz, C. Fulton, and R. D. Palmer, "Source current polarization impact on the cross–polarization definition of practical antenna elements: Theory and applications," *IEEE Trans. Antennas Propag.*, vol. 66, no. 9, pp. 4391–4406, Sep. 2018.

JORGE L. SALAZAR-CERRENO (Senior Member, IEEE) received the B.S. degree in ECE from University Antenor Orrego, Trujillo, Peru, the M.S. degree in ECE from the University of Puerto Rico, Mayagüez (UPRM), and the Ph.D. degree in ECE from the University of Massachusetts, Amherst, in 2011. His Ph.D. research focused on the development of low-cost dual-polarized active phased array antennas (APAA). At NCAR, he worked with the Earth Observing Laboratory (EOL) Division developing airborne technology for two-dimensional, electronically scanned, and dual-pol phased array radars for atmospheric research. In July 2014, he joined the Advanced Radar Research Center (ARRC), The University of Oklahoma, as a Research Scientist, where he became an Assistant Professor with the School of Electrical and Computer Engineering, in August 2015. His research interests include high-performance, broadband antennas for dual-polarized phased array radar applications, array antenna architecture for reconfigurable radar systems, APAA, Tx/Rx modules, radome EM modeling, and millimeter-wave antennas. He is a Senior Member of the IEEE Antennas and Propagation Society (AP-S) and a Reviewer of various IEEE and AMS conferences and journals. After graduation, he received the Prestigious National Center for Atmospheric Research (NCAR) Advanced Study Program (ASP) Postdoctoral Fellowship. In 2019, he received the prestigious William H. Barkow Presidential Professorship from The University of Oklahoma for meeting the highest standards of excellence in scholarship and teaching.

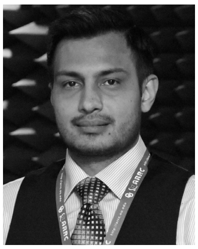

ZEESHAN QAMAR (Member, IEEE) received the B.Sc. and M.Sc. degrees in electrical engineering from COMSATS University, Islamabad, Pakistan, in 2010 and 2013, respectively, and the Ph.D. degree in electronic engineering from the City University of Hong Kong, Hong Kong, in 2017. From July 2010 to August 2013, he was a Research Associate with the Department of Electrical and Computer Engineering, COMSATS University. From November 2017 to April 2018, he was a Postdoctoral Research Associate with the Department of Materials Science and Engineering, City University of Hong Kong. He is currently a Postdoctoral Research Fellow with the Phased Array Antenna Research and Development Group (PAARD) and the Advanced Radar Research Center (ARRC), The University of Oklahoma, Norman, OK, USA. His current research interests include microwave/millimeter-wave circuits, material characterization, meta-materials, artificial dielectric layer, antennas and phased arrays, phased array antennas. He is a member of the IEEE Antennas and Propagation Society (AP-S) and a Reviewer of various IEEE and IET conferences and journals.

SHAHROKH SAEEDI (Senior Member, IEEE) received the B.Sc. and M.Sc. degrees (Hons.) in electrical engineering from the Iran University of Science and Technology, Tehran, Iran, in 1999 and 2002, respectively, and the Ph.D. degree in electrical and computer engineering from The University of Oklahoma, Norman, OK, USA, in 2015. From 2002 to 2011, he worked as an RF Design Engineer, a Senior Research and Development Engineer, and a Project Manager, where he was involved in RF/microwave sub-system and system design. He is currently a Research Associate and a Fabrication Lab Manager with the Advanced Radar Research Center, Norman, where he is involved in design of miniaturized microwave filters for integration with the next-generation of multifunction phased array radars. His other research interests include design of high-power reconfigurable and conformal antennas for agile radar systems, advanced filter synthesis for widely adaptable RF front-ends in cognitive radios and radar systems, microfluidic RF electronics, and rapid fabrication and additive manufacturing of microwave and millimeter wave structures. He was the Co-Founder and the Chair of the IEEE MTT-S Student Branch Chapter, The University of Oklahoma. He is a member of the IEEE Microwave Theory and Techniques Society (MTT-S) and the IEEE Antennas and Propagation Society (AP-S) and a Reviewer of various IEEE and IET conferences and journals. His research received several awards, including best student paper awards in 2019 IEEE Texas Symposium on Wireless and Microwave Components and Systems, 2018 IEEE International Symposium on Antennas and Propagation, 2019 and 2017 IEEE Wireless and Microwave Technology Conferences, and 2016 IEEE Radio Wireless Symposium.

BINBIN WENG (Member, IEEE) received the B.S. degree in physics from Xiamen University, in 2006, the M.S. degree in semiconductor physics from Zhejiang University, in 2008, and the Ph.D. degree in electrical and computer engineering from The University of Oklahoma (OU), in 2012. He is currently an Assistant Professor of Electrical and Computer Engineering with OU. His research focuses on numerical simulation, fabrication, and characterization of micro-/nano-scale photonic and electronic devices and systems. In the meantime, he also serves as the Director of Operations of the University's Microfabrication Research and Education Center, OU. He has authored or coauthored over 30 journal publications, three patent inventions, and conference contributions. He is a member of OSA.

HJALTI S. SIGMARSSON (Senior Member, IEEE) received the B.Sc. degree in electrical and computer engineering from the University of Iceland, Reykjavik, Iceland, in 2003, and the M.Sc. and Ph.D. degrees in electrical and computer engineering from Purdue University, West Lafayette, in 2005 and 2010, respectively. He is currently with the School of Electrical and Computer Engineering and the Advanced Radar Research Center (ARRC), The University of Oklahoma, Norman, OK, USA, where he is currently an Associate Professor. His current research is focused on reconfigurable RF and microwave hardware for agile communications, measurement, and radar systems. Furthermore, his research interests include spectral management schemes for cognitive radio architectures, advanced packaging utilizing heterogeneous integration techniques, and additive manufacturing of electromagnetic components. He was a recipient of the Best Paper Award of the IMAPS 2008 41st International Symposium on Microelectronics. In 2015, he received the Air Force Office of Scientific Research (AFOSR) Young Investigator Program (YIP) to support his research on reconfigurable high-frequency components using phase-change materials. He was named the recipient of the Gerald Tuma Presidential Professorship for meeting the highest standards of excellence in scholarship and teaching, in 2018.